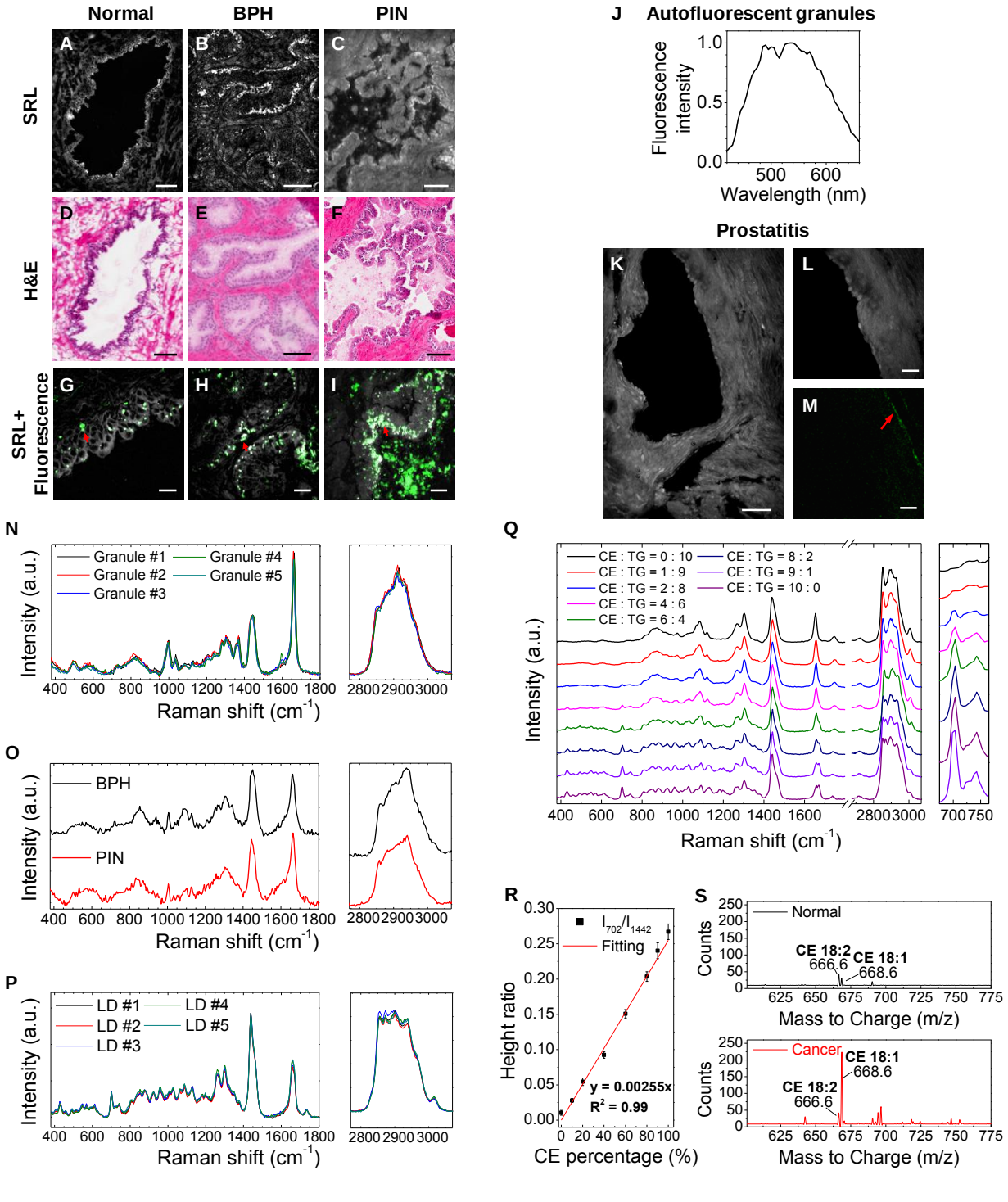
Normal
BPH
PIN
SRL
H&E
SRL+ Fluorescence
A
B
C
D
E
F
G
H
I
J
Autofluorescent granules
Fluorescence intensity
Wavelength (nm)
Prostatitis
K
L
M
N
Granule #1
Granule #2
Granule #3
Granule #4
Granule #5
Intensity (a.u.)
Raman shift (cm-1)
O
BPH
PIN
P
LD #1
LD #2
LD #3
LD #4
LD #5
Q
CE : TG = 0 : 10
CE : TG = 1 : 9
CE : TG = 2 : 8
CE : TG = 4 : 6
CE : TG = 6 : 4
CE : TG = 8 : 2
CE : TG = 9 : 1
CE : TG = 10 : 0
R
I702/I1442
Fitting
y = 0.00255x
R2 = 0.99
Height ratio
CE percentage (%)
S
Normal
Cancer
CE 18:2
666.6
CE 18:1
668.6
Counts
Mass to Charge (m/z)

Figure S1. Related to Figure 1. (**A-I**) Stimulated Raman loss (SRL) and two-photon fluorescence images of normal prostate, BPH, and PIN. (**A-C**) Large-area SRL images and (**D-F**) corresponding hematoxylin and eosin (H&E)-stained slides. Scalar bar, 100 μm. (**G-I**) High magnification SRL and two-photon fluorescence images of the lesions shown in (A-C) (grey: SRL, green: two-photon fluorescence). Autofluorescent granules indicated by red arrows. Scalar bar, 20 μm. (**J**) Normalized two-photon fluorescence spectrum of autofluorescent granule in normal prostate. (**K**) Large-area SRL image of prostatitis. Scalar bar, 100 μm. (**L, M**) High magnification SRL and two-photon fluorescence images of the selected area shown in (K) (grey: SRL, green: two-photon fluorescence). Red arrow indicates extracellular fibrous structures. Scalar bar, 20 μm. (**N**) Raman spectra of different autofluorescent granules in one normal prostate tissue. (**O**) Raman spectra of autofluorescent granules in BPH and PIN lesion. (**P**) Raman spectra of LDs in different cells in one PCa specimen. (**Q**) Raman spectra of CE/TG emulsions with eight different CE:TG molar ratios, ranging from 0:10 to 10:0. CE/TG emulsions are mixtures of cholesteryl oleate and glyceryl trioleate and used as the standards of certain CE molar percentage. Spectral intensity shown in (N-Q) was normalized by the peak at 1442 cm^{-1}. (**R**) Calibration curve for quantification of molar percentage of CE out of total neutral lipid, generated by linear fitting of height ratio between the peak at 702 cm^{-1} and the peak at 1442 cm^{-1}. Height ratio = 0.00255 × CE percentage (%). The intercept was set to 0 for linear fitting. (**S**) Mass spectra of lipids extracted from normal prostate and high-grade PCa tissues. m/z 666 and m/z 668 stand for cholesteryl linoleate (CE 18:2) and cholesteryl oleate (CE 18:1), respectively.

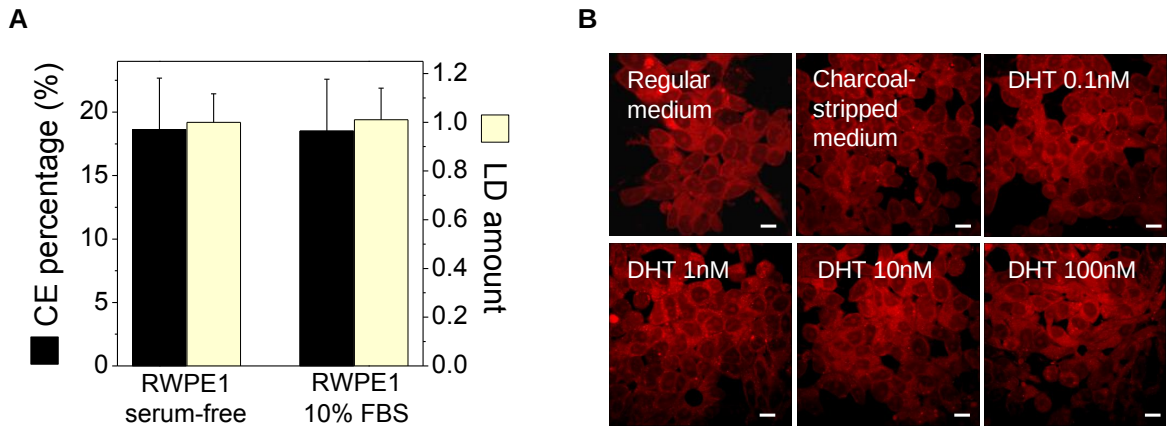

Figure S2. Related to Figure 2. (**A**) LD amount and CE percentage of RWPE1 cells cultured in regular serum-free medium and the medium supplemented with 10% FBS (fetal bovine serum). (**B**) SRL images of 22Rv-1 cells treated with different concentrations of dihydrotestosterone (DHT). DHT was diluted in phenol-red free RPMI + 10% charcoal-stripped serum, 4 days incubation. Scalar bar, 10 μm.

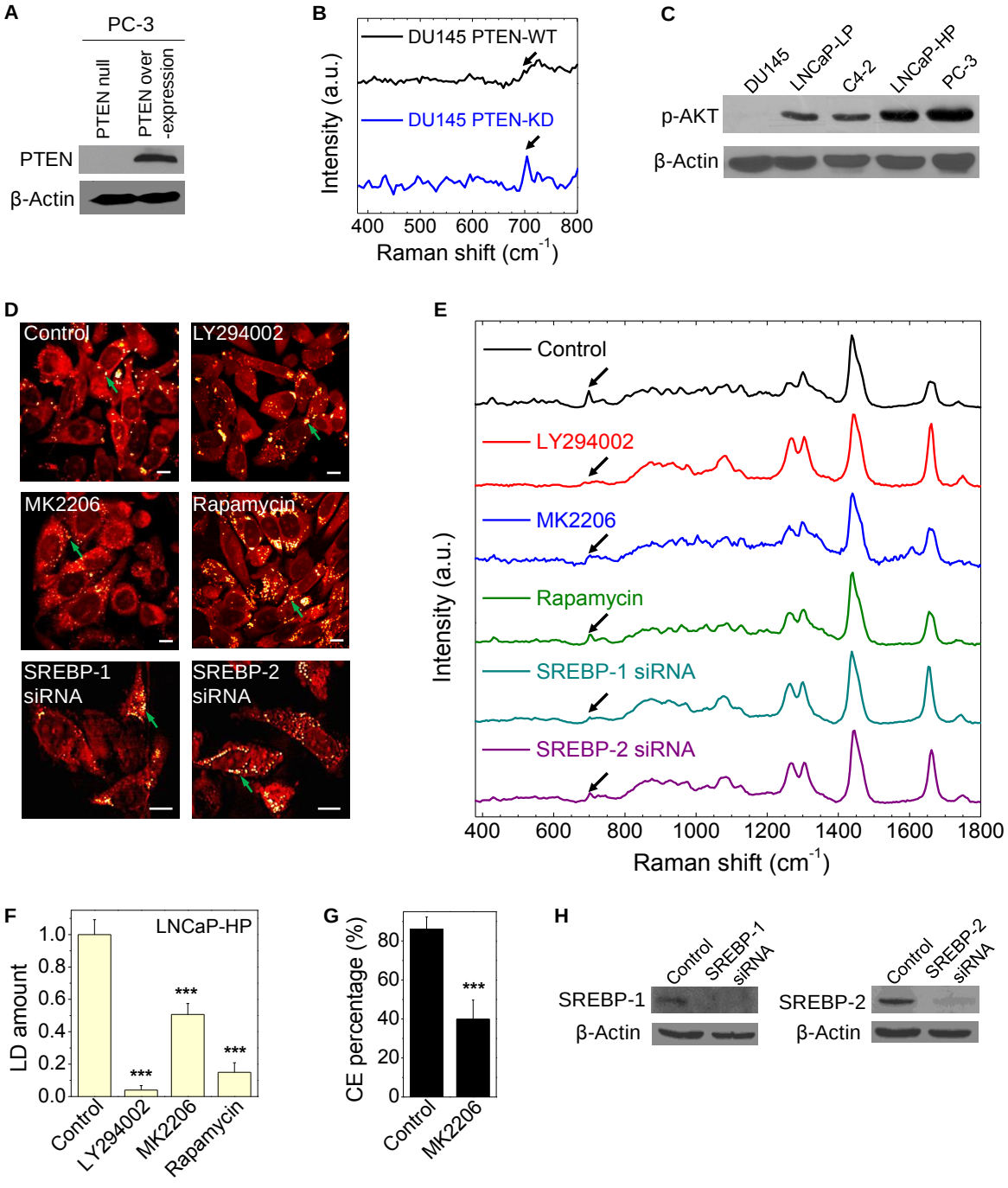
A
PC-3
PTEN null
PTEN over -expression
PTEN
β-Actin
B
DU145 PTEN-WT
DU145 PTEN-KD
Intensity (a.u.)
400 500 600 700 800
Raman shift (cm-1)
C
DU145
LNCaP-LP
C4-2
LNCaP-HP
PC-3
p-AKT
β-Actin
D
Control
LY294002
MK2206
Rapamycin
SREBP-1 siRNA
SREBP-2 siRNA
E
Control
LY294002
MK2206
Rapamycin
SREBP-1 siRNA
SREBP-2 siRNA
Intensity (a.u.)
400 600 800 1000 1200 1400 1600 1800
Raman shift (cm-1)
F
LNCaP-HP
LD amount
1.0 0.8 0.6 0.4 0.2 0.0
***
***
***
Control
LY294002
MK2206
Rapamycin
G
CE percentage (%)
80 60 40 20 0
***
Control
MK2206
H
Control
SREBP-1 siRNA
SREBP-1
β-Actin
Control
SREBP-2 siRNA
SREBP-2
β-Actin

Figure S3. Related to Figure 3. (**A**) Immunoblot of antibodies against PTEN and β-Actin in PTEN null and PTEN overexpressed PC-3 cells. (**B**) Raman spectra of LDs in PTEN-WT and PTEN-KD DU145 cells. Spectral intensity was normalized by the peak at 1442 cm^{-1}. The band of cholesterol rings at 702 cm^{-1} was significantly higher in the PTEN-KD DU145 cell compared to the PTEN-WT DU145 cell, as indicated by the arrows. (**C**) Immunoblot of antibodies against p-AKT and β-Actin in PCa cells, including LNCaP-LP, LNCaP-HP, C4-2, PC-3, and DU145. (**D**) SRL images of cells treated with DMSO as control, LY294002 (50 μM, 3 day), MK2206 (10 μM, 2 day), rapamycin (100 nM, 2 day), and SREBP-1 and -2 siRNA (2 day transfection). LDs indicated by green arrows. Scalar bar, 10 μm. (**E**) Raman spectra of LDs in PC-3 cells undergone the treatments shown in (D). Spectral intensity was normalized by the peak at 1442 cm^{-1}. The bands of cholesterol rings at 702 cm^{-1} were significantly reduced after the treatments, as indicated by the arrows. (**F**) LD amount and (**G**) CE percentage of LNCaP-HP cells treated with DMSO as control, LY294002 (50 μM, 3 day), MK2206 (10 μM, 2 day), and rapamycin (100 nM, 2 day). (**H**) Immunoblot of antibodies against SREBP-1 or -2 (precursor forms), and β-Actin in SREBP-1 or -2 siRNA-transfected PC-3 cells. WT: wild-type, KD: knockdown. Error bars represent SEM. ***: $p < 0.0005$.

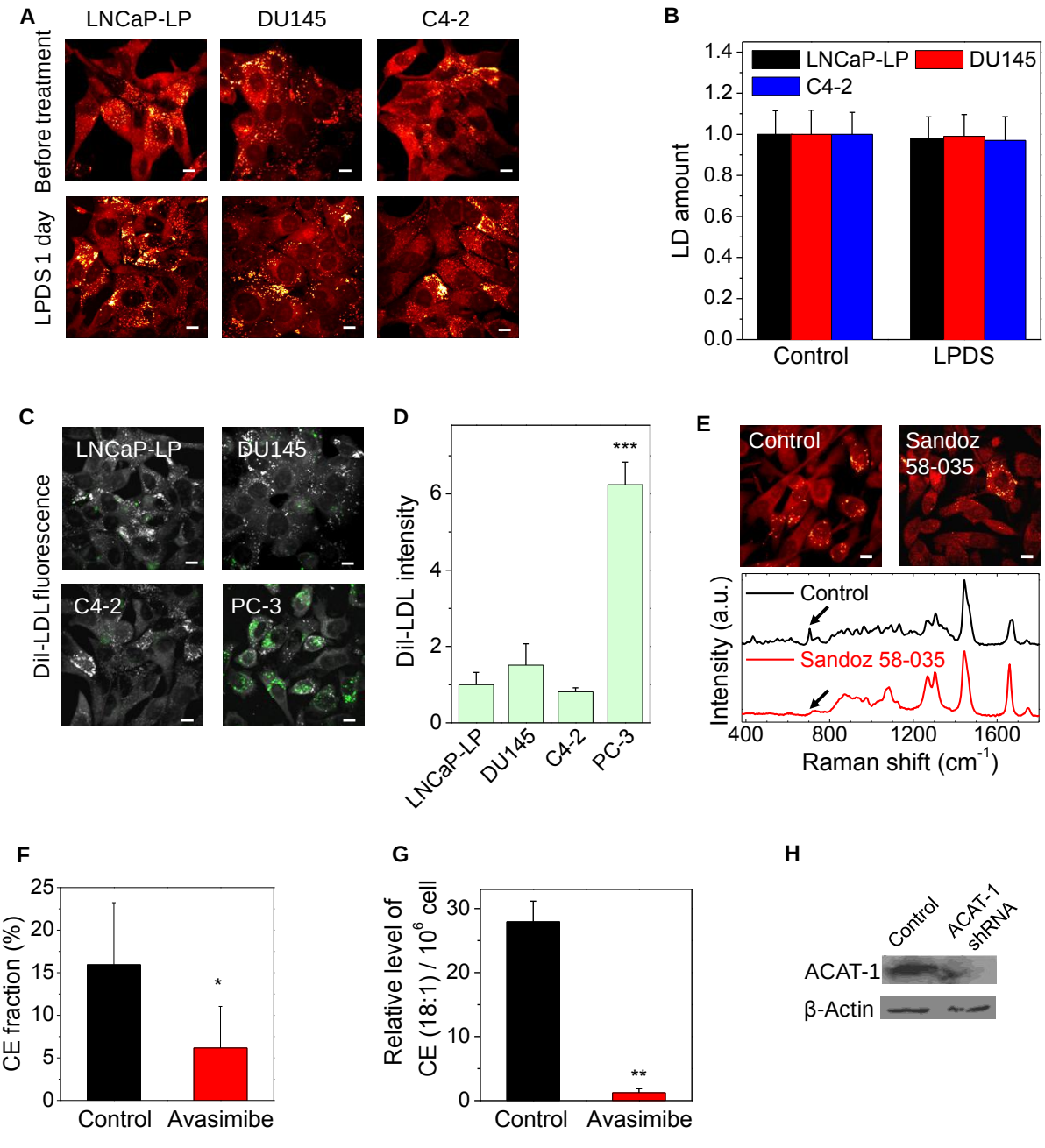
A
LNCaP-LP
DU145
C4-2
Before treatment
LPDS 1 day
B
LNCaP-LP
DU145
C4-2
LD amount
Control
LPDS
C
LNCaP-LP
DU145
C4-2
PC-3
Dil-LDL fluorescence
D
Dil-LDL intensity
***
LNCaP-LP
DU145
C4-2
PC-3
E
Control
Sandoz 58-035
Control
Sandoz 58-035
Intensity (a.u.)
Raman shift (cm-1)
F
CE fraction (%)
*
Control
Avasimibe
G
Relative level of CE (18:1) / 10^6 cell
**
Control
Avasimibe
H
Control
ACAT-1 shRNA
ACAT-1
β-Actin

Figure S4. Related to Figure 4. (**A-B**) Representative SRL images and quantitation of LD amount of various CE-poor cancer cells, including LNCaP-LP, DU145, and C4-2, before and after 1 day LPDS treatment. LD amounts in cells before treatments were normalized for each cell line. (**C-D**) Representative images and quantitation of DiI-LDL uptake in various cell lines, including LNCaP-LP, PC-3, DU145, and C4-2. DiI-LDL treatment: 20 μg/ml for 3 hours. Grey: SRL; Green: two-photon fluorescence of DiI-LDL. (**E**) SRL images and Raman spectra of LDs in PC-3 cells with and without Sandoz 58-035 treatment (10 μM, 1 day). Spectral intensity was normalized by the peak at 1442 cm^{-1}. The bands of cholesterol rings at 702 cm^{-1} nearly disappeared after the treatment, as indicated by the arrows. (**F**) Effect of avasimibe treatment (7.5 μM, 2 day) on fraction of CE out of total cholesterol in PC-3 cells, measured by biochemical assay. (**G**) Relative levels of cholesteryl oleate (CE 18:1) in control and avasimibe-treated PC-3 cells (7.5 μM, 2 day), measured by mass spectrometry and normalized by cell number (n = 3). (**H**) Immunoblot of antibodies against ACAT-1 and β-Actin in control and ACAT-1 shRNA-transfected PC-3 cells. Scalar bar = 10 μm. Error bars represent SEM. *: $p < 0.05$. **: $p < 0.005$, ***: $p < 0.0005$. LPDS: lipoprotein deficient serum; DiI-LDL: DiI-labeled LDL.

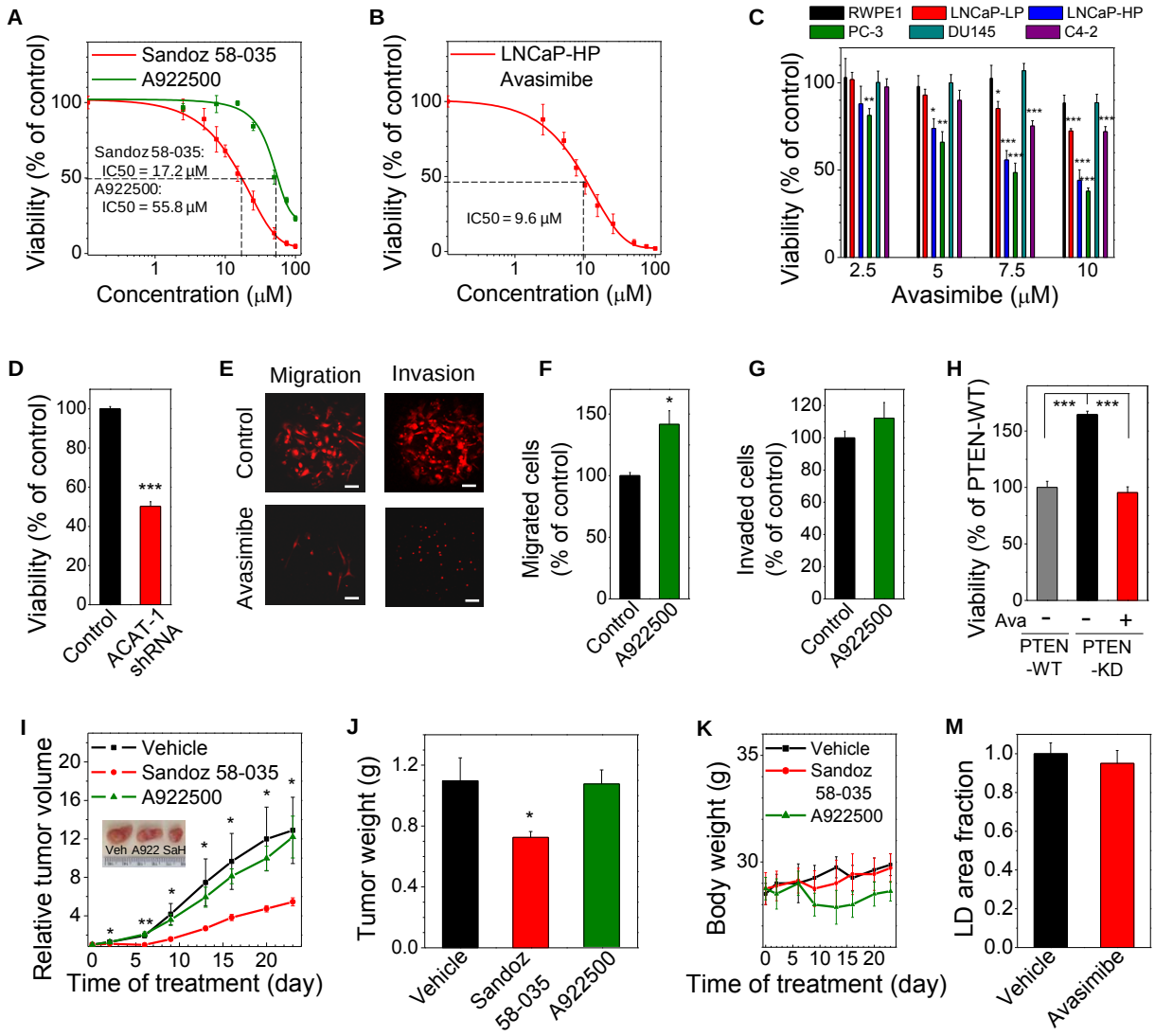
A
Sandoz 58-035
A922500
Viability (% of control)
Sandoz 58-035:
IC50 = 17.2 μM
A922500:
IC50 = 55.8 μM
Concentration (μM)
B
LNCaP-HP
Avasimibe
IC50 = 9.6 μM
C
RWPE1
LNCaP-LP
LNCaP-HP
PC-3
DU145
C4-2
Avasimibe (μM)
D
Control
ACAT-1 shRNA
E
Migration
Invasion
Control
Avasimibe
F
Migrated cells (% of control)
G
Invaded cells (% of control)
H
Viability (% of PTEN-WT)
Ava
PTEN -WT
PTEN -KD
I
Vehicle
Sandoz 58-035
A922500
Relative tumor volume
Time of treatment (day)
J
Tumor weight (g)
K
Body weight (g)
M
LD area fraction
L
Heart
Kidney
Liver
Lung
Spleen
Tumor
Ki67
TUNEL
Vehicle
Avasimibe

Figure S5. Related to Figure 5. (**A**) IC50 curves of Sandoz 58-035 (IC50 = 17.2 μM) and A922500 (IC50 = 55.8 μM) treatments (3 day) on PC-3 cells (n = 6 per group). (**B**) IC50 curve of avasimibe treatment (3 day) on LNCaP-HP cells (IC50 = 9.6 μM). n = 6 per group. (**C**) Viability of various cell lines, including RWPE1, LNCaP-LP, LNCaP-HP, PC-3, DU145, and C4-2, treated with different concentrations of avasimibe (2.5, 5, 7.5, and 10 μM, for 3 days). RWPE1 was cultured in media supplemented with 10% FBS for viability test. Viability is the percentage of viable cells in avasimibe-treated group compared to that in control group for each cell line. n = 6 per group. (**D**) Viability of PC-3 cells transfected with ACAT-1 shRNA for 3 days. n = 6 per group. The absorbance values measured for the control groups were used for normalization in (A-D). (**E**) Representative images of migration and invasion of PC-3 cells pre-treated with avasimibe (5 μM, 2 day). Red: propidium iodide staining. Scalar bar, 50 μm. Quantitation of migrated (**F**) and invaded (**G**) PC-3 cells pre-treated with DGAT-1 inhibitor A922500 (10 μM, 2 day), n = 3. The number of migrated or invaded cells in control groups was used for normalization. (**H**) Viability of PTEN wild-type (PTEN-WT) and PTEN knockdown (PTEN-KD) DU145 cells treated with avasimibe (7.5 μM) for 2 days. n = 6 per group. The PTEN-WT DU145 group was used for normalization. (**I**) Relative tumor volume of PC-3 xenograft (n = 8). Sandoz 58-035 and A922500 treatments started 2 weeks after tumor implantation (day 0), and were given daily via intraperitoneal injections at the doses of 15 mg/kg and 3 mg/kg, respectively. Relative tumor volume = tumor volume / initial tumor volume (day 0) for each mouse. Representative tumors harvested on day 23 are shown in the inset. Veh: vehicle, SaH: Sandoz 58-035, A922: A922500. (**J**) Weight of tumor tissues harvested from the mice in (I) (n = 8). (**K**) Body weight of mice over 23-day treatments (n = 8). (**L**) H&E staining of sections of heart, kidney, liver, lung, and spleen harvested at the end of the animal study (day 30) from hosts receiving intraperitoneal delivery of vehicle or avasimibe in Figure 5E. And representative images of H&E staining, immunohistochemistry of Ki67, and TUNEL labeling (blue: DAPI, cyan: TUNEL-positive) of tumor tissues harvested from the same animals shown in Figure 5E. Scalar bar, 100 μm. (**M**) Quantitation of LD area fraction of tumor tissues harvested from the same animals shown in Figure 5E (n = 5). Error bars represent SEM. *: $p < 0.05$. **: $p < 0.005$, ***: $p < 0.0005$.

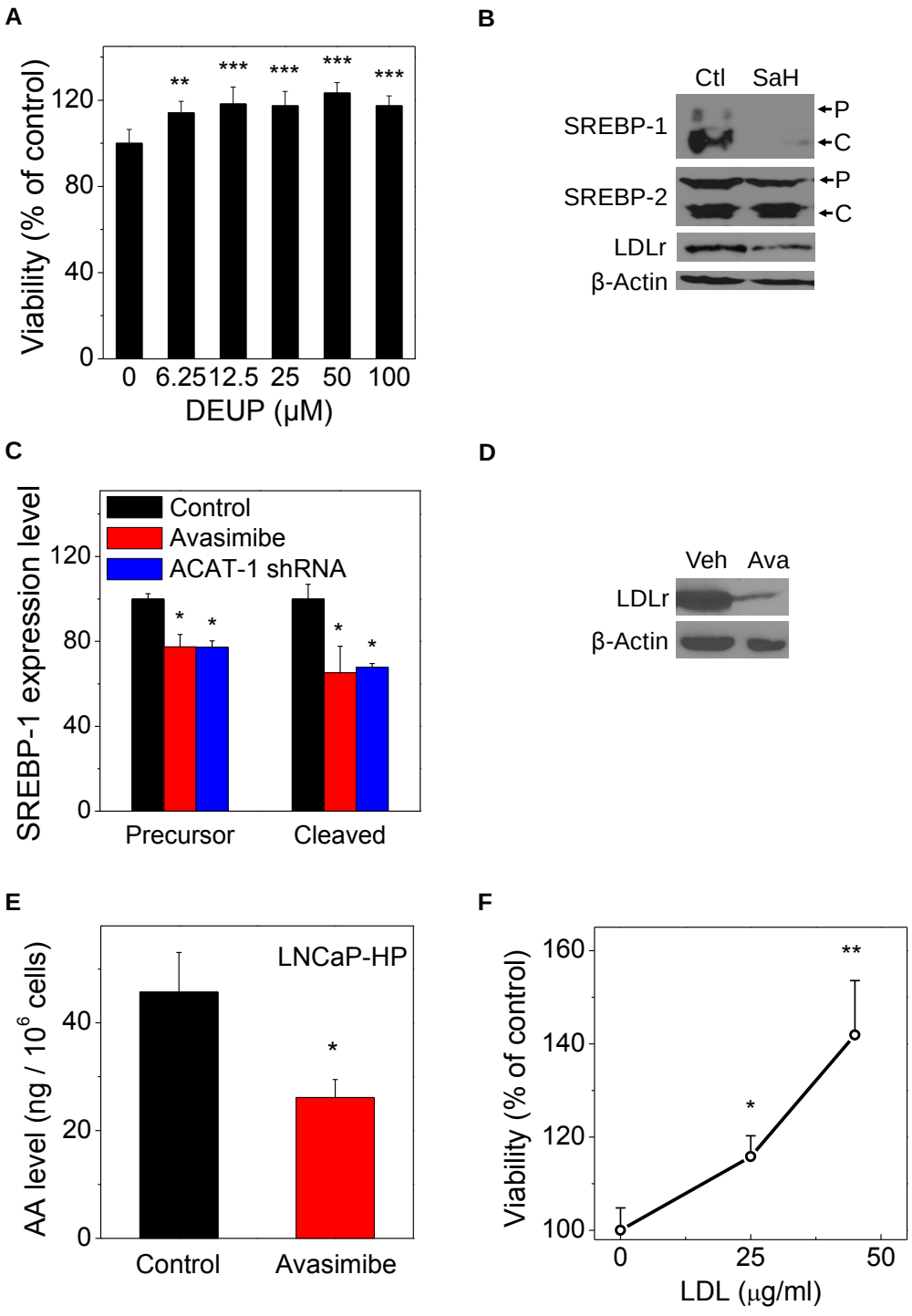
A
Viability (% of control)
120
80
40
0
**
***
***
***
***
0 6.25 12.5 25 50 100
DEUP (μM)
B
Ctl SaH
SREBP-1
P
C
SREBP-2
P
C
LDLr
β-Actin
C
SREBP-1 expression level
120
80
40
0
Control
Avasimibe
ACAT-1 shRNA
*
*
*
*
Precursor
Cleaved
D
Veh Ava
LDLr
β-Actin
E
AA level (ng / 10^6 cells)
40
20
0
LNCaP-HP
*
Control
Avasimibe
F
Viability (% of control)
160
140
120
100
**
*
0
25
50
LDL (μg/ml)

Figure S6. Related to Figure 6. (**A**) Viability of PC-3 cells treated with different concentrations of CE hydrolase inhibitor, diethylumbelliferyl phosphate (DEUP), for 3 days. n = 6 per group. (**B**) Immunoblot of antibodies against SREBP-1, -2, LDLr, p-AKT, and β-Actin in PC-3 cells treated with Sandoz 58-035 (SaH, 10 μM, 3 day). P: precursor form, C: cleaved form. (**C**) Relative expression levels of SREBP-1 precursor and cleaved forms in PC-3 cells upon ACAT-1 knockdown (ACAT-1 shRNA for 3 days) or ACAT inhibition (avasimibe, 7.5 μM, 2 day). (**D**) Immunoblot of antibodies against LDLr and β-Actin in PC-3 tumor tissues harvested from mice treated vehicle (Veh) or avasimibe (Ava). (**E**) AA levels in control and avasimibe-treated (7.5 μM, 2 day) LNCaP-HP cells (n = 3). (**F**) PC-3 cell viability upon LDL treatments (n > 6 per group). The absorbance values measured for control groups were used for normalization. Error bars represent SEM. *: $p < 0.05$, **: $p < 0.005$, ***: $p < 0.0005$.

Table S1. Related to Figure 1. Area fraction of LDs, presence of autofluorescent granules, and molar percentage of CE in LDs in prostate specimens from healthy donors and PCa patients.

	Autofluorescent granule	LD area fraction (%)	LD area fraction Mean ± SD[a](%)	CE percentage (%)	CE percentage Mean ± SD (%)
Normal [b] (n = 19)	All positive	ND [c]			
BPH (n = 10)	All positive	ND			
Prostatitis (n = 3)	All negative	ND			
PIN (n = 3)	All positive	ND			
Low-grade PCa (Gleason 3, n = 9) [d]	Negative	0.155	0.78 ± 0.65	69.9	90.2 ± 9.1
		1.376		97.7	
		0.527		94.2	
		0.146		88.1	
		0.709		101.3	
		0.998		92.6	
		2.084		84.0	
		0.145		92.6	
		0.909		91.6	
High-grade PCa (Gleason 4 or 5, n = 11) [e]	Negative	3.974	3.93 ± 1.74	84.0	90.6 ± 4.9
		2.466		99.6	
		6.094		86.1	
		4.831		88.5	
		4.940		83.5	
		1.830		93.2	
		3.275		94.5	
		3.030		91.3	
		6.391		89.1	
		1.100		91.7	
		5.279		94.6	
Metastases [f] (n = 9)	All negative	1.431	2.76 ± 1.19	89.0	70.3 ± 18.5
		3.998		82.0	
		3.006		44.6	
		4.311		42.4	
		3.364		60.7	
		3.622		82.8	
		0.996		60.6	
		2.364		82.9	
		1.710		88.1	

[a] SD = standard deviation

[b] Normal prostate tissues were collected from healthy donors (n = 3) and PCa patients (n = 16).

[c] ND = not detectable

[d] Borderline cases (Gleason 3): one tissue specimen does not have any lipid accumulation; two tissue specimens only contain autofluorescent granules but not LDs.

[e] Borderline case (Gleason 4 or 5): one tissue specimen only contain autofluorescent granules but not LDs.

[f] Metastases: liver (n = 2), lymph node (n = 3), rib (n = 1), lung (n = 1), adrenal (n = 1), and abdominal soft tissue (n = 1).

Table S2. Related to Figure 2. Origin, AR expression, androgen dependence, and PTEN status in various human prostate cells.

Cell lines	Origin	AR [a] expression	Androgen dependence	PTEN
RWPE1	Normal prostate	+	Dependent	Normal
LNCaP-LP [b]	Lymph node metastasis	+	Dependent	Mutated
LNCaP-HP [c]	Lymph node metastasis	+	Independent	Mutated
PC-3	Bone metastasis	-	Independent	Deleted
DU145	Brain metastasis	-	Independent	Normal
C4-2	Derivative of LNCaP-LP by passing through castrated mice	+	Independent	Mutated
22Rv-1	Derivative of CWR22 (primary prostate cancer cell) by passing through castrated mice	+	Independent	Normal

[a] AR: androgen receptor
[b] LNCaP-LP: low passage LNCaP cell (passage number < 20).
[c] LNCaP-HP: high passage LNCaP cell (passage number > 60).

Supplemental Experimental Procedures:

Human prostate tissue specimens

This study was approved by institutional review board. Frozen specimens of human prostate tissues derived from patients who underwent radical prostatectomy for PCa were obtained from Indiana University Simon Cancer Center Solid Tissue Bank. These patients had not received hormone therapy before radical prostatectomy. In addition, frozen specimens of normal prostate tissues donated from healthy subjects and metastatic PCa tissues collected by warm body autopsy from patients who had failed hormone therapy were obtained from Johns Hopkins Hospital. Totally, 19 normal prostates, 10 BPH, 3 prostatitis, 3 PIN lesions, 12 low-grade PCa (Gleason grade 3), 12 high-grade PCa (Gleason grade 4 or 5), and 9 metastatic PCa [liver (n = 2), lymph node (n = 3), rib (n = 1), lung (n = 1), adrenal (n = 1), and abdominal soft tissue (n = 1)] from 64 different patients or healthy donors were analyzed. For each tissue specimen, pairs of neighboring slices were prepared, with one slice remained unstained for spectroscopic imaging and the other stained with H&E. Pathological examination was made by genitourinary pathologists.

Cell culture

Keratinocyte Serum Free Medium (K-SFM) with additives bovine pituitary extract (BPE) and human recombinant epidermal growth factor (hEGF), RPMI 1640, T-medium, and fetal bovine serum (FBS) were purchased from Invitrogen. F-12K and EMEM were obtained from American Type Cell Collection (ATCC). Cells were cultured in the following media: RWPE1 in K-SFM supplemented with BPE (0.05 mg/ml) and hEGF (5 ng/ml). LNCaP-LP, LNCaP-HP, and 22Rv-1 in RPMI 1640 supplemented with 10% FBS. PC-3 in F-12K supplemented with 10% FBS. DU145 in EMEM supplemented with 10% FBS. C4-2 in T-medium supplemented with 10% FBS. LNCaP-HP was derived upon continuous passage from original LNCaP from ATCC (LNCaP-LP) until the passage number was over 60, and is an established cell line of AR-positive but androgen-independent PCa (Igawa et al., 2002; Lin et al., 2003; Unni et al., 2004; Youm et al., 2008).

Chemicals

LY294002, MK2206, rapamycin, avasimibe, simvastatin, Sandoz 58-035, DEUP, cholesteryl oleate, glyceryl trioleate, A922500, puromycin, polybrene, DHT, and AA were purchased from Sigma-Aldrich. Human LDL was obtained from Creative Laboratory Products. LPDS was purchased from Biomedical Technologies. The PTEN inhibitor BPV(pic) was purchased from Enzo Life Sciences.

Label-free Raman spectromicroscopy

Average acquisition time for a 512 x 512 pixels SRL image was 1.12 second. Large-area SRL imaging was performed on a motorized stage. Each large-area SRL image was generated by stitching 100 images of ~157 μm × 157 μm in size together. Two different locations were imaged for each specimen. Simultaneously, backward-detected two-photon fluorescence signal was collected through a 520/40 nm bandpass filter for the imaging of autofluorescent granules.

The background of Raman spectrum was removed as described (Slipchenko et al., 2009). 5-10 spectra of LDs or autofluorescent granules in 5-10 different cells were taken for each specimen. Each Raman spectrum ranged from 380 to 3100 cm^{-1} and was acquired in 20 seconds.

The laser (~707 nm) power at the specimen was maintained at 15 mW, and no cell or tissue damage was observed.

Fluorescence imaging of LDL uptake

DiI-labeled LDL (DiI-LDL)was made using dry film method (de Smidt and van Berkel, 1990). Cells in growth medium containing 10% lipoprotein deficient serum with or without the indicated inhibitors (for 2d) were incubated with DiI-LDL (20 μg/ml) for 3 hr at 37 ℃ and then imaged by two-photon fluorescence microscopy through a 600/60 nm bandpass filter. The LDL uptake was quantified based on fluorescence intensity of DiI using ImageJ, and normalized by cell number. No LDL uptake was detected in cells incubated at 4 ℃.

Cell viability assay

Cells were grown in 96-well plates (~5000 cells/well) and cultured for 1 day followed by indicated treatments. Cell viability was measured with the MTT colorimetric assay (Sigma). IC50 was obtained by fitting the data with sigmoidal dose response model.

Cell cycle analysis

PC-3 cells treated with 7.5 μM avasimibe for 3 days and the untreated ones were collected, fixed, and stained with 50 μg/ml propidium iodide (PI) at 37 ℃ for 30 min. The DNA content was measured by Cytomics FC500 flow cytometer (Beckman Coulter). Data were processed and analyzed by FlowJo software (Tree Star). Cell-cycle phases and frequencies of each phase were determined by fitting the data with Watson-Pragmatic model.

Migration and invasion assays

Invasion and migration assays were performed in Transwell chambers (Corning) with 8 μm pore-sized membranes, coated with and without Matrigel (BD Bioscience) respectively. One to two days before the start of the assays, cells received indicated treatments. At the start of the assays, cells were harvested and counted. 1×10^6 cells were seeded in the upper chamber of the transwells in 1.5 ml serum-free media. The media in lower chamber contain 20% FBS. Cells were allowed to migrate for 12 hr and invade for 24 hr at 37 °C. The transwell membranes were then fixed and stained with PI. Cells that had not migrated or invaded through the chamber were removed with a cotton swab. The cells that migrated or invaded were imaged by two-photon fluorescence microscopy, and 4 fields were independently counted from each migration or invasion chamber. An average of cells in 4 fields for one migration or invasion chamber represents n = 1.

Electrospray ionization mass spectrometry (ESI-MS) measurement of lipid extraction

Lipid extraction from cell pellets and tissues was performed according to Folch *et al* (Folch et al., 1957). Cells with indicated treatments were collected and counted. ESI-MS analysis was conducted according to the protocol described previously (Liebisch et al., 2006). The relative level of cholesteryl oleate (18:1) was normalized by cell number for comparison between control and avasimibe-treated cells, and was normalized by tissue weight for comparison between normal prostate and prostate cancer tissues.

Biochemical measurement of cellular lipids

Lipids were extracted as described above. CE, free cholesterol, and TG concentrations were measured according to the manufacturer's protocol (Amplex Red Cholesterol kit from Molecular Probes, Serum Triglyceride Determination Kit from Sigma), and finally normalized by protein content that was determined by bicinchoninic acid assay.

Liquid chromatography-mass spectrometry (LC-MS) analysis of AA

Cells cultured in 10% LPDS were pre-treated with 7.5 μM avasimibe for 2 days or transfected with ACAT-1 shRNA for 3 days. LDL (20 μg/ml) were then added back to the medium for 6 hr before the cells were collected and counted. Fatty acids were extracted and measured according to the methods described previously (Yang et al., 2007). The final AA concentration was normalized by cell number.

Immunoblotting

After indicated treatments, cells were lysed in AMI lysis buffer (Active Motif), and proteins were detected by immunoblotting with the antibodies against SREBP-1 (BD Pharmingen, 557036), SREBP-2 (Santa Cruz, sc-5603), p-AKT (Cell Signaling, 4060L), p-S6 (Cell Signaling, 2211L), LDLr (Millipore, MABS26), ACAT-1 (Santa Cruz, sc-69836), and β-actin (Sigma, A5441). The western blots were quantified using the Gel Analysis functions in the software ImageJ. β-actin was used as loading control for normalization.

Immunohistochemistry (IHC)

Murine paraffin-embedded slides were deparaffinized and rehydrated. Then antigens were retrieved in antigen unmasking solution (Vector Laboratories) with a 2100-Retriever (PickCell Laboratories). Samples were then incubated with the antibody against Ki67 (Abcam, ab16667) or subjected to TUNEL assay (Roche, 11684817910).

RNA interference

RNA interference was employed to specifically deplete endogenous SREBP-1, SREBP-2, ACAT-1, and PTEN. Plasmids pLKO.1-SREBP-1 and pLKO.1-SREBP-2 were constructed with the targeting sequences CAACCAAGACAGUGACUUCCC and CAACAGACGGUAAUGAUCACG. The ACAT-1 shRNA plasmid and PTEN shRNA lentiviral particle were purchased from Santa Cruz (sc-29624-SH, sc-29459-V). Plasmid DNA was transfected with Lipofectamine®2000 (Invitrogen 11668030) as described in the manufacturer's protocols. PTEN shRNA lentiviral particle was introduced into cells with 5 μg/ml polybrene. Stable transfected cell line was selected using 2 μg/ml puromycin. Control shRNA (nonspecific) was used as control for indicated shRNA.

Treatment of PCa in mouse xenograft models

The protocol for this animal study was approved by the Purdue Animal Care and Use Committee. Tumor cells ($2\sim3 \times 10^6$) were mixed with an equal volume of Matrigel (BD Bioscience) and inoculated subcutaneously into the right flank of 6-week-old athymic nude mice (Harlan Laboratories). Treatments started 2 weeks after tumor implantation when the xenografts were about ~100 mm^3 (day 0). Inhibitors were dissolved in DMSO, diluted with the solvent PBS containing 1% Tween-80, and administrated via daily intraperitoneal injections for 20~30 days at the dose of 15 mg/kg for avasimibe and Sandoz 58-035, and at the dose of 3 mg/kg for A922500. The dosages for injections were selected based on previous animal studies on these inhibitors

(Llaverías et al., 2003; Williams et al., 1989; Zhao et al., 2008). The reason that the dosage of A922500 is lower than that of Sandoz 58-035 and avasimibe is A922500 has substantially lower IC50 compared to Sandoz 58-035 or avasimibe for inhibition of the target enzyme, that is, IC50 of A922500 to inhibit DGAT-1 is ~7 nM vs. IC50 of Sandoz 58-035 and avasimibe is ~3.3 μM (Lee et al., 1996; Rodriguez and Usher, 2002; Zhao et al., 2008). Tumor volume, estimated from the formula: $V=L\times W^2/2$ (V: volume, mm^3; L: length, mm; W: width, mm), was measured twice a week with digital calipers. Relative tumor volume = tumor volume / initial tumor volume (measured on day 0), for each mouse. Body weight was also measured twice a week. Tumors and major organs, including heart, liver, lung, kidney, and spleen, were harvested and prepared for tumor weight measurement, spectroscopic imaging, H&E, and IHC staining.

Statistical analysis

Results of LD area fraction and CE percentage in human prostate tissues were shown as mean ± standard deviation (SD). Other results were shown as mean ± standard error of the mean (SEM). One-way ANOVA was used for comparisons of LD area fraction, LD amount, and CE percentage among different lesion types of human PCa and different treatment conditions of cell cultures. All other comparisons that only include two groups in cellular and animal studies were performed using the Student's t test. $p < 0.05$ was considered statistically significant.

Supplemental References:

de Smidt, P.C., and van Berkel, T.J.C. (1990). Prolonged serum half-life of antineoplastic drugs by incorporation into the low density lipoprotein. Cancer Res. 50, 7476-7482.

Lee, H.T., Sliskovic, D.R., Picard, J.A., Roth, B.D., Wierenga, W., Hicks, J.L., Bousley, R.F., Hamelehle, K.L., Homan, R., Speyer, C., et al. (1996). Inhibitors of acyl-CoA:cholesterol O-acyl transferase (ACAT) as hypocholesterolemic agents. CI-1011: an acyl sulfamate with unique cholesterol-lowering activity in animals fed noncholesterol-supplemented diets. J. Med. Chem. 39, 5031-5034.

Lin, H.K., Hu, Y.C., Yang, L., Altuwaijri, S., Chen, Y.T., Kang, H.Y., and Chang, C.S. (2003). Suppression versus induction of androgen receptor functions by the phosphatidylinositol 3-kinase/Akt pathway in prostate cancer LNCaP cells with different passage numbers. J. Biol. Chem. 278, 50902-50907.

Rodriguez, A., and Usher, D.C. (2002). Anti-atherogenic effects of the acyl-CoA:cholesterol acyltransferase inhibitor, avasimibe (CI-1011), in cultured primary human macrophages. Atherosclerosis 161, 45-54.

Unni, E., Sun, S.H., Nan, B.C., McPhaul, M.J., Cheskis, B., Mancini, M.A., and Marcelli, M. (2004). Changes in androgen receptor nongenotropic signaling correlate with transition of LNCaP cells to androgen independence. Cancer Res. 64, 7156-7168.

Williams, R.J., McCarthy, A.D., and Sutherland, C.D. (1989). Esterification and absorption of cholesterol: in vitro and in vivo observations in the rat. Biochim. Biophys. Acta. 1003, 213-216.

Youm, Y.H., Kim, S., Bahk, Y.Y., and Yoo, T.K. (2008). Proteomic analysis of androgen-independent growth in low and high passage human LNCaP prostatic adenocarcinoma cells. BMB Rep. 41, 722-727.

Zhao, G., Souers, A.J., Voorbach, M., Falls, H.D., Droz, B., Brodjian, S., Lau, Y.Y., Iyengar, R.R., Gao, J., Judd, A.S., et al. (2008). Validation of diacyl glycerolacyltransferase I as a novel target for the treatment of obesity and dyslipidemia using a potent and selective small molecule inhibitor. J. Med. Chem. 51, 380-383.